Synthesis and Characterization of Ordered, Very Large Pore MSU-H Silicas Assembled from Water-Soluble Silicates

Seong Su Kim, Abhijeet Karkamkar, and Thomas J. Pinnavaia*,†

Department of Chemistry and Center for Fundamental Materials Research, Michigan State University, East Lansing, Michigan 48824

Michal Kruk and Mietek Jaroniec*,‡

Department of Chemistry, Kent State University, Kent, Ohio 44240

Received: February 28, 2001; In Final Form: June 18, 2001

Two-dimensional, hexagonally ordered silicas with large uniform mesopores (7.6−11.9 nm) have been assembled through a nonionic supramolecular assembly pathway using sodium silicate as a silica source and the triblock copolymer Pluronic P123 ($EO_{20}PO_{70}EO_{20}$) as a structure-directing agent. An increase in the synthesis temperature from 308 to 333 K in a one-step procedure led to a systematic increase in the unit-cell size, pore diameter, specific surface area, and pore volume, and to a decrease in the pore wall thickness. The resulting materials exhibited adsorption properties highly similar to those of SBA-15 silica assembled through an electrostatic pathway under strongly acidic conditions, indicating that the framework structure of MSU-H is analogous to that of SBA-15 and consists of ordered large pores connected by micropores in the pore walls. When the one-step synthesis procedure was followed by a post-assembly hydrothermal treatment at 373 K, the resultant MSU-H silicas exhibited framework pores enlarged by 1.7−2.8 nm and substantially increased secondary (textural) porosity, a feature that is not characteristic of SBA-15. These results demonstrated a wide range of possibilities in tailoring the structures of silicas synthesized using low-cost and convenient reagents. In addition, gas adsorption data for the MSU-H silicas allowed us to examine the accuracy of a recently proposed procedure for calculation of the pore size distributions, calibrated using MCM-41 silicas and extrapolated over larger pore sizes. It was found that this procedure overestimates pore diameters for MSU-H silicas, which might be related to the inaccuracy of the aforementioned extrapolation, or to deviations of the MSU-H pore shape from uniform cylindrical pores with the length much larger than the pore diameter.

1. Introduction

Over the last several years, the synthesis of mesoporous materials via oligomer or polymer templating[1,2] has become increasingly popular. In particular, there has recently been much interest in the preparation of ordered mesoporous silicas.[2−12] These materials can readily be functionalized by grafting of inorganic species,[13,14] deposition of metal particles,[15] and chemical bonding of organosilanes,[16−20] and are useful as catalysts,[13,15] and adsorbents for heavy metal ions,[19,20] and proteins.[16] Immobilization of proteins in the porous structure of polymer-templated silica was also achieved.[21] After proper doping, polymer-templated silicas are promising as lasers,[22] photochromic[23] and photosensitive[24] materials, and pH sensors.[25] Moreover, porous structures of polymer-templated silicas have attracted much interest as templates for the synthesis of metal nanowires,[26−29] ordered bundles of metal nanowires,[29,30] ordered mesoporous carbons,[31] silicon nanowires,[32] and polymer coaxial nanocables.[33]

Because of the many prospective applications of oligomer- and polymer-templated silicas, there has been a need for the development of cost-effective approaches for their synthesis. Polymer templates themselves are inexpensive and can be readily recovered using solvent extraction.[1,4] The synthesis can be accomplished at relatively low temperatures, often ambient,[1,4] and rarely above 373 K.[4] The time necessary to self-assemble a polymer-templated silica can be as short as 5−20 h in the case of conventional synthesis,[1,34] 2 h or less in the case of microwave-assisted hydrothermal synthesis,[35,36] and several seconds in the case of evaporation-induced self-assembly.[7] However, until recently all of the reported oligomer- and polymer-templated syntheses of mesoporous materials required expensive inorganic precursors, such as tetraethyl orthosilicate (TEOS), as noted by Kwon et al.[34] and Sierra and Guth.[37] These authors proposed to use alternative, cost-effective inorganic precursors, such as H_2SiF_6[34] or sodium silicate.[37] However, the resulting disordered silicas had quite broad pore size distributions, as seen from the reported gas adsorption data, and those obtained from sodium silicate exhibited low thermal stability. Later, thermally stable oligomer-templated silicas with wormlike porous structures similar to those obtained using TEOS were synthesized using sodium silicate as a silica source.[38,39] The pore size of the silicas synthesized using the low-cost silica source could be tailored in the same manner as in the case of materials synthesized using the expensive TEOS,[8,40] that is via temperature control within a range from 298 to 333 K,[38] or addition of fluoride,[39] and without compromising the ability to tailor the morphology of porous silica particles.[39] More recently, two brief reports were published[12,41] on the synthesis of various

* Corresponding authors.
† E-mail: pinnavai@cem.msu.edu.
‡ Phone: (330) 672 3790. Fax: (330) 672 3816. E-mail: jaroniec@columbo.kent.edu.

10.1021/jp010773p CCC: $20.00
Published on Web 07/20/2001

ordered porous silicas and mesocellular silica foams[42] using sodium silicate and oligomeric or polymeric templates under acidic[41] and nearly neutral[12] pH conditions. The synthesis of polymer-templated two-dimensionally (2-D) hexagonally ordered silicas under conditions close to neutral (these materials are denoted herein MSU-H) is particularly appealing from both a practical and fundamental point of view. This is because the formation of ordered silica-surfactant structures under these convenient synthesis conditions has not been reported unless: (i) certain electrolytes, such as fluoride salts[8−10] or metal salts,[6] are purposefully added, sometimes in combination with the use of a rapidly hydrolyzing silica source (tetramethyl orthosilicate (TMOS)),[9] or (ii), as-synthesized sample is subjected to the hydrothermal treatment in water (in the case of some oligomeric templates only).[5] The purpose of the present work was to further explore the opportunities in the MSU-H synthesis. Two series of MSU-H silicas were synthesized using one-step and two-step procedures (the latter being reported for the first time herein) and the resulting materials were thoroughly characterized using X-ray diffraction (XRD), transmission electron microscopy (TEM), and nitrogen adsorption. The pore size adjustment by controlling the synthesis temperature and the tailoring of textural porosity through the postsynthesis hydrothermal treatment are discussed herein. Moreover, the MSU-H silicas were employed as model adsorbents to study capillary condensation/evaporation. The results of this fundamental adsorption study are reported and their practical implications are briefly discussed.

2. Materials and Methods

2.1. Materials. Samples of MSU-H were prepared using either a one-step or a two-step assembly process using sodium silicate as the silica source (27% SiO_2, 14% NaOH) and Pluronic P123 as the nonionic structure-directing triblock copolymer surfactant. In the one-step process,[12] the mesostructure was formed at a fixed assembly temperature of 308, 318, or 333 K. The surfactant and an amount of acetic acid equivalent to the hydroxide content of the sodium silicate solution were mixed at ambient temperature and then added to the sodium silicate solution to form a reactive silica in the presence of the structure directing surfactant. This allowed for the assembly of the hexagonal framework under pH conditions where both the silica precursor and the surfactant were primarily nonionic molecular species (pH = ~6.5). The reaction time was 20 h, and the overall reaction stoichiometry was 1.00 Si/0.017 P123/230 H_2O. In the two-step process, the one-step process was repeated and then the reaction temperature was increased to 373 K for an additional 20 h. The solid products were filtered, washed with water, and dried in air. To completely remove the surfactant, the as-synthesized products were calcined in air at 873 K. The samples obtained using the one-step and two-step procedures are denoted MSU-H-*x* and MSU-H-*x*P, respectively, where *x* is the absolute temperature of the first synthesis step.

2.2. Measurements. Nitrogen adsorption measurements were carried out at 77 K using a Micromeritics ASAP 2010 volumetric adsorption analyzer. Prior to the measurements, the samples were outgassed under vacuum at 473 K in the port of the adsorption analyzer. X-ray diffraction (XRD) patterns of powdered samples were obtained on a Rigaku Rotaflex diffractometer equipped with a rotating anode and Cu Kα radiation. Transmission electron microscopy (TEM) was carried out on a JEOL 100CX instrument using an electron beam generated by a CeB_6 filament and an acceleration voltage of 120 kV. Samples for TEM studies were prepared by dipping a carbon-coated copper grid into a suspension of mesoporous material in ethanol that was sonicated for 10 min.

2.3. Methods. The BET specific surface area, S_{BET},[43] was calculated from nitrogen adsorption data in a relative pressure range from 0.04 to 0.2. The total pore volume[43] (that is the volume of pores of size below about 200 nm) was determined from the amount adsorbed at a relative pressure of about 0.99. The primary pore volume, V (defined here as the volume of primary mesopores, V_p, and micropores, V_{mi}), and the external surface area, S_{ex}, were calculated using the α_s plot method[43,44] from data in the α_s range from 1.6 to 2 for MSU-H (308) and 1.75−2.15 for MSU-H (318) and (333). It should be noted that α_s is the standard relative adsorption defined as the amount adsorbed as a function of relative pressure divided by the amount adsorbed at a relative pressure of 0.4 for the reference adsorbent. In general, pores are classified herein on the basis of their diameter as micropores (<2 nm), mesopores (2−50 nm), and macropores (>50 nm).[43] However, because MSU-H samples are structurally similar to SBA-15 and thus exhibit a broad distribution of micropores and mesopores of the size close to the micropore range,[30] we will use the term "micropores" to denote all these relatively narrow pores, keeping in mind that some of them may actually be beyond the micropore range. The micropore volume[43,44] was estimated using α_s plot method in the α_s range from 0.9 to 1.1 for MSU-H (308) and from 0.9 to 1.2 for all other samples. A macroporous silica LiChrospher Si-1000 was used as a reference adsorbent,[45] and its BET surface area evaluated in the relative pressure range from 0.04 to 0.2 was 26.4 $m^2\ g^{-1}$. The pore size distribution (PSD) was evaluated using the method calibrated for a series of MCM-41 silicas with pore sizes from 2 to 6.5 nm, as described elsewhere.[46] The pore size was also evaluated using an equation derived on the basis of geometrical considerations of the structure of a material, whose porosity consists of an array of uniform channels arranged in a 2-D hexagonal pattern, and disordered smaller pores in the pore walls.[47] This structure is characteristic of SBA-15 silica. It was stated in the original report on the MSU-H synthesis using a one-step procedure that thus synthesized MSU-H is structurally similar to SBA-15.[12] As will be discussed later, the current study provides an additional confirmation of this identification.

Under the assumptions outlined above, the pore size, w_d, can be assessed on the basis of the XRD (100) interplanar spacing, d_{100}, the volume of primary mesopores, V_p, and the volume of micropores, V_{mi}:

$$w_d = cd_{100}\left(\frac{V_p}{1/\rho + V_p + V_{mi}}\right)^{1/2} \quad (1)$$

where c is a constant whose value is dependent on the pore geometry and is equal to 1.213 for cylindrical pores, and ρ is the density of pore walls (assumed to be equal to that of amorphous silica, that is 2.2 g cm^{-3}).[47]

3. Results and Discussion

3.1. X-ray Diffraction. Figure 1 provides XRD patterns for representative MSU-H silica mesostructures prepared by a nonionic supramolecular pathway from sodium silicate and P123 surfactant in a one-step assembly process at 333 K (MSU-H-333). Included in the figure is the pattern for the product formed from a two-step process involving framework assembly at 333 K, followed by a post-assembly hydrothermal treatment at 373 K (MSU-H-333P). Mesostructures prepared by analogous one- and two-step processes at initial framework assembly temperatures of 308 and 318 K exhibited the same number of diffraction lines. The corresponding d_{100} values are listed in

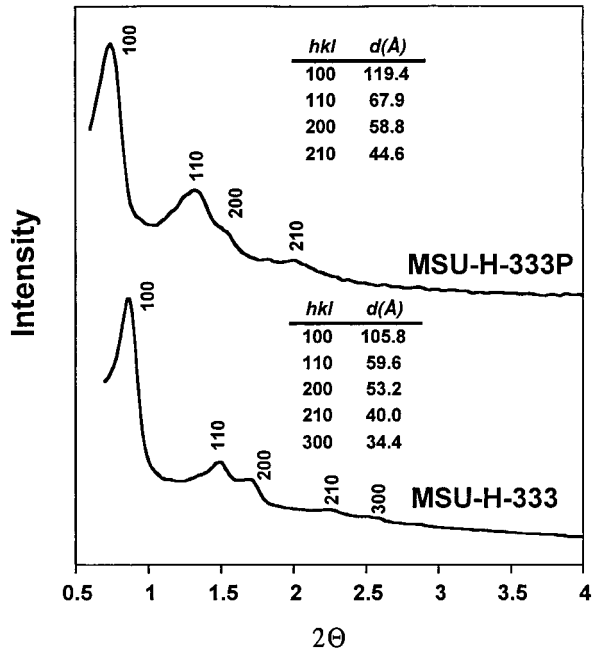

Figure 1. Powder XRD patterns for selected MSU-H silicas synthesized using the one-step and two-step synthesis.

TABLE 1: Structural Parameters of MSU-H Silicas

sample	(*100*) interplanar spacing (nm)	BET specific surface area ($m^2\ g^{-1}$)	total pore volume ($cm^3\ g^{-1}$)	pore diameter[a] (nm)
MSU-H-308	9.2 (11.4)	530	0.62	7.6
MSU-H-318	9.9 (12.1)	710	0.91	8.9
MSU-H-333	10.6 (12.6)	870	1.25	10.2
MSU-H-308P	10.9 (11.3)	520	1.49	10.4
MSU-H-318P	11.6 (12.0)	500	1.31	11.6
MSU-H-333P	11.9 (12.6)	530	1.35	11.9

[a] Interplanar *100* spacing of the samples calcined at 873 K for 4 h; the values in parentheses are the interplanar spacings for the as-synthesized samples. [b] The pore diameter was assessed using eq 1; for, MSU-H-*x*P samples, see the text for the assumptions made concerning the calculations.

Table 1. Included in the Table are the spacings observed for the as-made products prior to surfactant removal by calcination. The *100* interplanar spacings for the as-synthesized samples, which increased systematically with increasing assembly temperature, were somewhat larger than those typically observed for SBA-15 silicas prepared by electrostatic assembly under strongly acidic conditions from the same polymer template and TEOS as a silica source.[3,4] The increase in *100* interplanar spacing with temperature, which was observed for calcined MSU-H silicas is reminiscent of the reported behavior of SBA-15.[3,4] The calcination led to a significant unit-cell size decrease (~2 nm), bringing the *100* interplanar spacings for the samples from the one-step assembly within the range typically observed for SBA-15 synthesized using the same polymer template using TEOS. However, the unit-cell parameter reported for SBA-15 synthesized from sodium silicate at 313 K and subsequently 373 K was smaller than that for MSU-H synthesized at temperatures much lower than 373 K (that is, 318 and 333 K). This suggests that unit-cell sizes achievable using the triblock copolymer template and sodium silicate are higher in the case of nearly neutral assembly conditions, when compared to strongly acidic conditions. The postsynthesis treatment at 373 K had essentially no effect on the *100* interplanar spacing for as-synthesized samples. However, the hydrothermal treatment clearly stiffened the framework, as evidenced by the magnitude

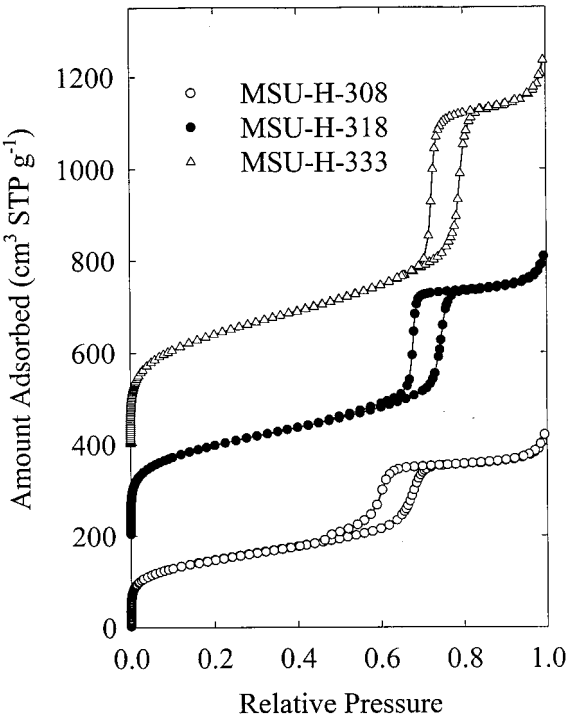

Figure 2. Nitrogen adsorption isotherms for MSU-H silicas synthesized using the one-step procedure.

of the contraction in *100* spacings upon removing the surfactant. Namely, the mesostructures subjected to the post-assembly hydrothermal treatment exhibited a substantially smaller lattice contraction (~0.5 nm) in comparison to those not subjected to hydrothermal treatment, as expected for a more completely cross-linked framework. Consequently, the pore sizes for the samples subjected to the post-assembly hydrothermal treatment were 1.7−2.8 nm larger than those observed for the mesostructures obtained from a one-step assembly process (see Table 1). We also note here that as-made MSU-H samples synthesized using the one-step procedure[12] showed the ratio of fully condensed (Q^4) $Si(OSi)_4$ sites to incompletely condensed Q^3 and Q^2 sites to be 4.5, considerably higher than the value of 1.28 reported for SBA-15 silicas.[3]

3.2. Nitrogen Adsorption and TEM. Nitrogen adsorption isotherms for the MSU-H samples are shown in Figures 2 and 3. The values of the BET specific surface area, total pore volume and pore diameter (calculated using eq 1) are listed in Table 1. As can be seen in Figure 2, adsorption isotherms for MSU-H samples synthesized using the one-step procedure are similar to those reported for SBA-15.[3,4,48] Moreover, the adsorption capacity increased and the position of the capillary condensation step shifted to higher relative pressures as the synthesis temperature increased, in the same manner as in the case of SBA-15 synthesized at different temperatures.[3,4,48] The specific surface areas, pore volumes, and pore diameters are also in the range typical for SBA-15 synthesized from TEOS[3,4] and sodium silicate.[41]

To further investigate the structural similarity between the porous structure of SBA-15 and MSU−H, a relation between the primary pore volume ($V = V_p + V_{mi}$), the primary pore surface area ($S = S_{BET} - S_{ex}$) and the primary mesopore diameter (w) of the MSU-H samples was examined. In principle, $wS/V = w(S_{BET} - S_{ex})/(V_p + V_{mi})$ is equal to 4.0 in the case of cylindrical pores. However, when one attempts to evaluate this quantity on the basis of experimental data, errors involved in the determination of w, S, and V, and perhaps some other factors,

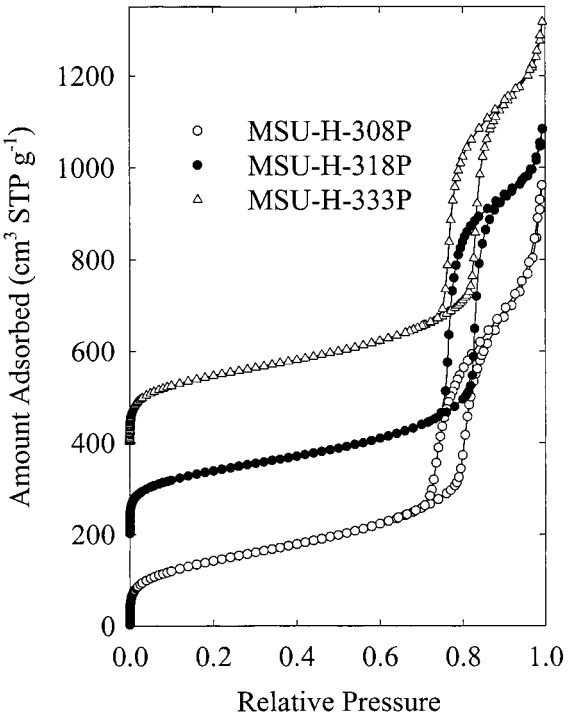

Figure 3. Nitrogen adsorption isotherms for MSU-H silicas synthesized using the two-step procedure involving a post-assembly hydrothermal treatment.

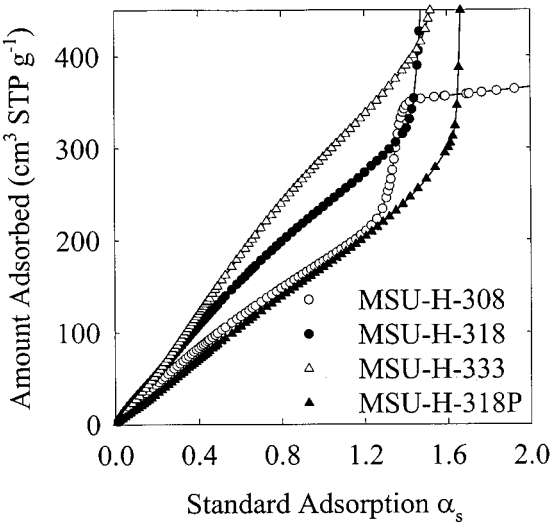

Figure 4. Initial parts of the α_s plots for selected MSU-H silicas.

such as surface roughness, cause the observed *wS*/*V* value to deviate from the theoretical value. In particular, in the case of structural parameters evaluated in the way analogous to that employed in the current study, a *wS*/*V* value between 4.5 and 5.0 is often observed for silicas with uniform, disconnected pore channels.[49] These materials include MCM-41 silica[50] as well as SBA-15 silica that has been calcined at 1173−1273 K in order to eliminate the connecting pores between ordered large pores.[49] In contrast, SBA-15 silica calcined at temperatures below 1173 K (the most commonly used calcination temperature is about 823 K)[3,4] exhibits $wS/V > 5.0$,[30,49] which is indicative of the presence of connecting porosity with a broad distribution extending from the micropore range toward the lower limit of the mesopore range.[30,49] The presence of these pores of size significantly smaller than those characteristic of the ordered mesopores of SBA-15 results in a larger specific surface area corresponding to a given pore volume, because smaller pores have larger ratios of surface area to pore volume for a given pore geometry, thus raising the *wS*/*V* factor above 5.0.

Calculations of *wS*/*V* for MSU-H samples obtained using a one-step synthesis actually provide *wS*/*V* values similar to those observed for SBA-15 calcined at a similar temperature, that is, 7.1, 7.4, and 7.4 for MSU-H-308, -318, and -333, respectively. As could be expected from these quite high values of the *wS*/*V* factor, MSU-H samples synthesized using a one-step procedure are microporous to some extent. The α_s plot analysis provided micropore volumes of 0.05, 0.08, and 0.09 cm^3 g^{-1} for MSU-H-308, -318, and -333, respectively. The α_s plots for these samples are shown in Figure 4. After an initial increase corresponding to a combination of the filling of micropores and monolayer−multilayer adsorption on the surface of primary mesopores, the slope of the plots decreases to some extent and segments of relatively good linearity can be observed for α_s values from 0.6−0.8 to 1.2−1.4, depending on the particular sample. These segments can be attributed to multilayer adsorption on the surface of primary mesopores and therefore are suitable for calculation of the micropore volume. However, it needs to be kept in mind that this multilayer formation process may be affected to some extent by both the presence of micropore openings on the surface of the primary mesopores and by enhanced adsorption in the proximity of the relative pressure of capillary condensation in primary mesopores. Both of these factors may lead to inaccuracy in the micropore volume determination. Indeed, the studies of SBA-15 silicas that exhibit similar shape of α_s plots suggests that the micropore volume derived as described above is underestimated,[51] although we are unable to determine the exact magnitude of this underestimation. The α_s values corresponding to the onset of the aforementioned linear segments of α_s plots increased as the synthesis temperature increased (about 0.55, 0.65 and 0.70 for MSU-H-308, -318, and -333 samples, respectively). This suggests that the filling of the micropores extended to higher relative pressures for samples synthesized at higher temperature. Since the micropore filling pressure is an increasing function of the pore size, it can be inferred that the distribution of the micropores shifts or tails toward somewhat larger pore sizes as the synthesis temperature is increased, as previously suggested to be the case for SBA-15 silicas.[48]

The α_s plots exhibited a steep rise at α_s above 1.4−1.6 that was related to the filling of primary mesopores, and subsequently leveled off after these pores had been filled with the condensed adsorbate (see α_s plot for MSU-H-308 in Figure 4). The subsequent linear segment of the α_s plot corresponds to multilayer adsorption on the external surface of particles of MSU-H. Only at α_s values above 2 was there some evidence of slight upward deviations of the plots due to capillary condensation in interparticle pores. This suggests that the phenomena of capillary condensation in primary mesopores and in interparticle (secondary) pores are well-separated and thus the former pores are of much smaller diameter than the latter. As expected from the α_s plots, PSDs for MSU-H silicas synthesized in the one-step process exhibited distinct peaks on the borderline between the micropore and mesopore ranges, similar to SBA-15 silicas (see Figure 5).[30,48] The PSD featured prominent sharp peaks centered between 7.5 and 11 nm corresponding to ordered porosity in the materials. The pore size increased as the synthesis temperature increased, which is reminiscent of the behavior of SBA-15.[3,4,48] However, the pore diameter achieved for MSU-H synthesized at 318 and 333 K was found to be comparable or higher than that for SBA-15 synthesized under acidic conditions using the same block copolymer template at a higher temperature (373 K).[3,4,48] This

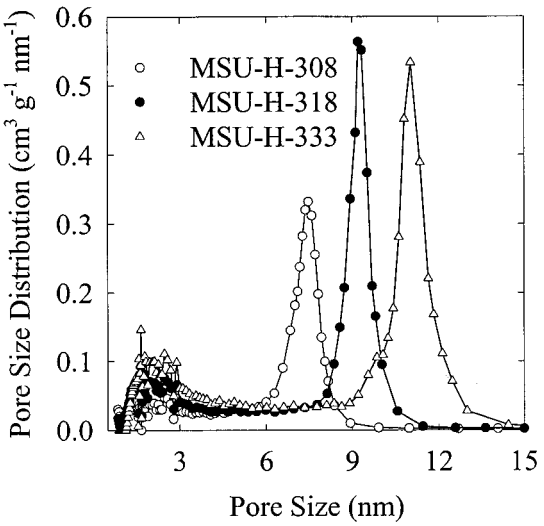

Figure 5. Pore size distributions for MSU-H silicas synthesized using the one-step procedure.

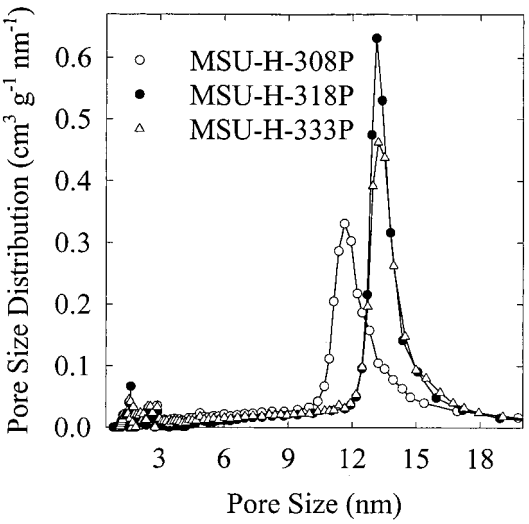

Figure 6. Pore size distributions for MSU-H silicas synthesized using the two-step procedure involving a post-assembly hydrothermal treatment at 373 K.

indicates that the assembly under nearly neutral pH conditions is capable of affording larger pore diameters a given temperature, when the same block copolymer is used. From the previous studies of SBA-15, one can expect that the tails between the peaks corresponding to ordered mesopores and the peaks on the borderline between micropore and mesopore ranges (see Figure 5) are artifacts of the calculation procedure.[30]

The results presented above strongly suggest that MSU-H silica synthesized using one-step synthesis appears to be SBA-15 analogue as far as the framework pore structure is concerned, although it needs to be kept in mind that framework properties of MSU-H are somewhat different, which manifests itself in a higher degree of framework condensation.[12] Moreover, MSU-H samples appear to have somewhat larger external surface areas (70, 90, and 150 m^2 g^{-1}, for the sample synthesized at 308, 318, and 333 K, respectively), which is likely to be related to the fact that the fundamental domain size of MSU-H is smaller than that of SBA-15 (see below).

The postsynthesis hydrothermal treatment of MSU-H led to major changes in the structure of the material. Except for the sample initially prepared at the lowest temperature, the treatment brought about a major decrease in the BET specific surface area. Moreover, the overall shape of the adsorption isotherms changed, because the amount adsorbed for the hydrothermally treated samples was increasing quite steeply even at relative pressures above those corresponding to the sharp steps of the capillary condensation in primary mesopores (see Figure 3). This indicates that appreciable secondary mesoporosity developed during the hydrothermal treatment step of the two-step synthesis process. Similar changes were not observed for SBA-15 hydrothermally treated at 373 K in a similar manner.[3,4,48] The absence of a clear separation between the filling of primary mesopores and the further increase in adsorption caused by multilayer formation and capillary condensation on the surface of secondary (textural) pores indicates that the secondary pores are of diameter much less than 1 order of magnitude larger than the primary (framework) pores of MSU−H subjected to the postsynthesis treatment. This can also be seen on PSDs, which exhibited tailing in the direction of larger pore sizes (see Figure 6).

The presence of substantial complementary textural porosity in MSU-H mesostructures, even when assembled in a one-step process, is verifiable by TEM. As shown in Figure 7A for the MSU-H-333 sample, the assembled particles are aggregates of intergrown fundamental domains a few hundred nanometers in size. The regions between the domains represent the textural mesopores that contribute to the nitrogen uptake beyond the filling of the framework pores at relative pressures above 0.90 (see Figure 2). Subjecting the assembled structures to a post-assembly hydrothermal treatment resulted not only in an enlargement of the framework pores, but also it appears to lead to the increase in the population of textural pores that exhibited a wide range of sizes (see Figure 7B). Moreover, it seems that the hydrothermally restructured material exhibited a broader distribution of sizes of fundamental domains. In particular, the projections of some of these domains along the incident electron beam were just several unit cells in width. These observations are in good agreement with the gas adsorption data discussed above, although a detailed comparison is certainly difficult due to the local nature of structural information attainable from TEM and to global averaged nature of information from gas adsorption. It appears that the structural changes upon the hydrothermal treatment of MSU-H are somewhat different from those observed for HMS silicas synthesized via a nonionic pathway using primary amines as structure-directing agents.[52] In the case of the latter, the Oswald ripening of the fundamental particles was observed. In the case of MSU-H silicas, a similar phenomenon is not clearly apparent, and since a fraction of fundamental domains of decreased size was observed after the hydrothermal treatment, a certain degree of degradation of fundamental domains to provide smaller particles might have taken place. Finally, it should be noted that the presence of intraparticle textural porosity is an intrinsic feature of MSU-H materials. In contrast, structurally equivalent SBA-15 mesostructures usually assemble into more monolithic particles with little or no textural porosity even after hydrothermal treatment.

The PSD curves shown in Figure 6 indicate that the post-assembly hydrothermal treatment also largely reduced the amount of micropores in the structure of MSU-H. However, the micropores are still likely to be present in the pore walls of these materials, because the α_s plot analysis indicated their small, yet detectable amount for the samples synthesized at two higher initial temperatures (about 0.02 cm^3 g^{-1} for both MSU-H-318P and -333P). Although α_s plot method did not provide evidence of micropores in MSU-H-308P silica, the presence of a certain amount of micropores still cannot be precluded, as inferred from earlier studies of SBA-15.[51] Previous studies of silicas templated

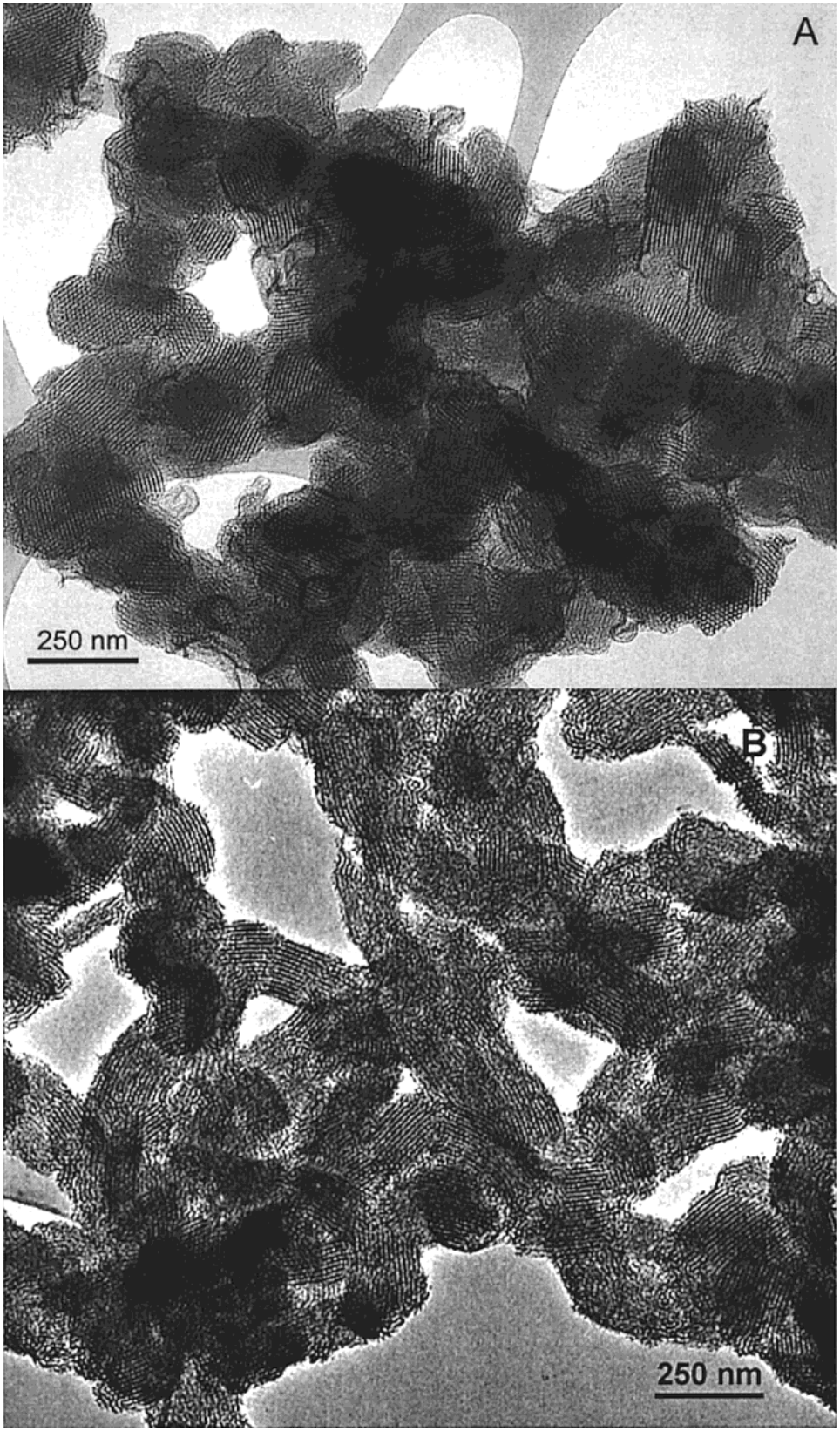

Figure 7. TEM images of the calcined forms of (A) MSU-H-333 and (B) MSU-H-333P showing a textured particle formed by the intergrowth of fundamental domains.

using diblock and triblock copolymer surfactants with poly(ethylene oxide) blocks, such as the P123 triblock copolymer used herein, suggested that the presence of micropores is a common feature of these materials.[30,53] So, the possibility of a reduction of the micropore volume during the postsynthesis hydrothermal treatment is certainly interesting, but it is rather unlikely that the microporosity was completely eliminated and thus the resulting structure is of MCM-41 type (disconnected channels arranged in a 2-D hexagonal pattern) rather than of SBA-15 type (channels arranged in 2-D hexagonal pattern and connected via small pores in the walls). Unfortunately, it does not seem possible to assess the wS/V factor, because of the

difficulty in the assessment of the primary pore volume and surface area. For materials obtained from the one-step procedure, it was possible to determine these quantities from the α_s plot and BET data. However, in the case of MSU-H synthesized using a two-step procedure, the slope of the α_s plot after the completion of the capillary condensation step corresponded to unrealistically large external surface area. This indicated that the aforementioned part is attributable to both multilayer adsorption and capillary condensation and therefore unsuitable for the assesesment of the pore volume and surface area with acceptable accuracy. Further studies would be required to provide a definite answer about the presence of micropores and the connectivity of primary pores in MSU−H synthesized using the two-step procedure.

It is known that in the case of 2-D hexagonally ordered mesoporous materials, the pore size and pore wall thickness can be evaluated from pore volume data (for instance, from gas adsorption) and the (100) interplanar spacing (for instance, from XRD).[46−48] For MSU-H silicas, one needs to account for the presence of micropores, presumably in the pore walls. In this case, eq 1 is applicable. It should be noted that in the case of the samples synthesized using the two-step procedure, an accurate determination of the primary pore volume was not possible, and reasonable, but somewhat arbitrary values of this quantity were assumed (0.75 $cm^3\ g^{-1}$ for MSU-H-308P and 1.00 $cm^3\ g^{-1}$ for MSU-H-318P and -333P). It can be readily demonstrated that even if the pore volume assumed were as much as 25% off from the actual value, only a small (about 4−5% in the case of MSU-H-318P) error in the pore diameter estimate would result because of the nature of eq 1 (for extensive discussion, see ref 47). The resulting pore size estimates are listed in Table 1. These estimates were used along with the unit-cell parameters (the distance between pore centers equal to $2 \times 3^{-1/2} d_{100}$) to evaluate the pore wall thickness of MSU-H. In the case of MSU-H-308, -318, and -333, the wall thickness was calculated to be 3.0, 2.5, and 2.1 nm. These values are similar to those determined for SBA-15 using similar calculation procedure.[48] However, in the latter study, a simplified form of eq 1 was used that did not take into consideration the microporosity in pore walls and consequently the pore wall thickness was likely to be underestimated therein. Clearly, the pore wall thickness decreased and the pore diameter increased as the synthesis temperature increased. This behavior has been observed for oligomer-[40] and polymer-templated silicas,[3,4,38,48] as well as for silicas synthesized using nonionic amines under near-neutral pH conditions.[52] The pore size enlargement was also observed after the postsynthesis treatment (see Table 1). This enlargement was accompanied by the pore wall thickness decrease to about 2.2 nm in the case of MSU-H-308P and to about 1.8 nm in the case of MSU-H-318P and MSU-H-333P.

Finally, some comments need to be made about an accuracy of the pore size estimates discussed so far. These estimates were derived using a relation between the capillary condensation pressure and the pore size derived using MCM-41 materials with pore sizes from 2 to 6.5 nm and further extrapolated over the entire mesopore range using the Kelvin equation with the statistical film thickness correction and an additional empirical correction.[46] This procedure provided pore size estimates of 7.5, 9.3, and 11.0 nm for MSU-H-308, -318, and -333, respectively. For the first two samples, these estimates are in acceptable agreement with the pore sizes calculated using eq 1 (see Table 1). However, the pore size estimated from gas adsorption using the aforementioned procedure for MSU-H-333 appears to be too large. The pore size evaluated for MSU-H-308P, -318P, and -333P appear to be even more overestimated (the values of 11.6, 13.1, and 13.6 nm were obtained, which are close to the unit-cell size of the materials and thus overestimated by at least 1 nm, compare with results in Table 1 that were obtained using eq 1) So, it appears that the method calibrated using MCM-41 silicas with pore sizes from 2 to 6.5 nm and extrapolated for larger pore sizes overestimated the pore sizes for the MSU-H samples with larger unit-cell sizes, and thus the obtained pore diameters would suggest an unrealistically small pore wall thickness (assessed as a difference between the unit-cell size and the pore size). This inability to determine the actual primary pore size of MSU-H with larger pores may be related to the inadequacy of the extrapolation of the relation between the pore diameter and the capillary condensation pressure over the pore sizes above 6.5 nm. Alternatively, it may be related to the deviations of the shape of primary pores of MSU-H from approximately cylindrical. These deviations may be caused by the presence of micropores in the pore walls. It has been reported recently that the capillary condensation between nanoscale contacts depends not only on their separation, but also on their size and shape.[54] A decrease in the size of the contacts delayed the capillary condensation for a given separation. Therefore, it can be expected that the presence of holes (micropores) in pore walls may lead to capillary condensation at a relative pressure somewhat higher than that for a pore of the same diameter that would not exhibit holes in its walls. Furthermore, in the case of the samples synthesized using the two-step procedure, the length of the pores may be equal only to several pore diameters, which could potentially lead to further shift in the capillary condensation pressure to higher relative pressures in comparison to the pore of much larger length/diameter ratio. Therefore, in the case of MSU-H silicas, the capillary condensation may take place at relative pressures somewhat higher than those expected for uniform siliceous cylindrical pores of the same size. The pore size calculation procedure calibrated on pores that were closer to the ideal shape and with larger length/diameter ratios would not account for this pressure shift and would incorrectly produce overestimated pore sizes. Further studies are needed to assess the accuracy of pore size distribution calculations for large mesopores using the method discussed herein.[46]

4. Conclusions

The synthesis of 2-D hexagonally ordered silicas using sodium silicate and triblock copolymer template under synthesis conditions that allow for nonionic supramolecular assembly pathway, provide much opportunity for the tailoring of the framework pore size and intraparticle textural porosity. The pore size can be adjusted by choosing an appropriate initial synthesis temperature. Further pore size enlargement can be achieved during the postsynthesis hydrothermal treatment. The framework pore structure of MSU-H appears to be similar to that of SBA-15 and therefore is likely to consist of ordered pores connected via micropores in the pore walls. The postsynthesis treatment at 373 K stiffens the framework while preserving some microporosity, although there is a decrease in the micropore volume. The hydrothermal treatment also appears to enhance the intraparticle textural porosity. These textural pores what may be beneficial in applications where accessibility of the porous structure is an issue, for instance in some catalytic processes.

Because of its periodic structure with uniform very large pores, MSU-H can be employed to test the relations between the pore diameter and capillary condensation pressure. It was found that the recently proposed relation calibrated using MCM-

41 silicas and extrapolated over pore sizes above 7 nm overestimates the pore diameter of MSU-H silicas with $d_{100} >$ 10 nm, and therefore similar results can be expected for SBA-15 of similar unit-cell size. It is yet to be verified if this overestimation is related to the inaccuracy of the extrapolated relation or to the finite length and deviations of the MSU-H pore shape from ideal cylindrical geometry.

Acknowledgment. The support of this research by NSF-CRG grant CHE-9903706 (T.J.P.) and NSF grant CTS-0086512 (M.J.) is gratefully acknowledged.

References and Notes

(1) Bagshaw, S. A.; Prouzet, E.; Pinnavaia, T. J. *Science* **1995**, *269*, 1242.
(2) Attard, G. S.; Glyde, J. C.; Goltner, C. G. *Nature* **1995**, *378*, 366.
(3) Zhao, D.; Feng, J.; Huo, Q.; Melosh, N.; Fredrickson, G. H.; Chmelka, B. F.; Stucky, G. D. *Science* **1998**, *279*, 548.
(4) Zhao, D.; Huo, Q.; Feng, J.; Chmelka, B. F.; Stucky, G. D. *J. Am. Chem. Soc.* **1998**, *120*, 6024.
(5) Bagshaw, S. A. *Chem. Commun.* **1999**, 271.
(6) Zhang, W.; Glomski, B.; Pauly, T. R.; Pinnavaia, T. J. *Chem. Commun.* **1999**, 1803.
(7) Lu, Y.; Fan, H.; Stump, A.; Ward, T. L.; Rieker, T.; Brinker, J. C. *Nature* **1999**, *398*, 223.
(8) Boissiere, C.; Larbot, A.; van der Lee, A.; Kooyman, P. J.; Prouzet, E. *Chem. Mater.* **2000**, *12*, 2902.
(9) Kim, J. M.; Han, Y.-J.; Chmelka, B. F.; Stucky, G. D. *Chem. Commun.* **2000**, 2437.
(10) Bagshaw, S. A. *J. Mater. Chem.* **2001**, *11*, 831.
(11) Yang, S. M.; Coombs, N.; Ozin, G. A. *Adv. Mater.* **2000**, *12*, 1940.
(12) Kim, S.-S.; Pauly, T. R.; Pinnavaia, T. J. *Chem. Commun.* **2000**, 1661.
(13) Cheng, M.; Wang, Z.; Sakurai, K.; Kumata, F.; Saito, T.; Komatsu, T.; Yashima, T. *Chem. Lett.* **1999**, 131.
(14) Luan, Z.; Maes, E. M.; van der Heide, P. A. W.; Zhao, D.; Czernuszewicz, R. S.; Kevan, L. *Chem. Mater.* **1999**, *11*, 3680.
(15) Kim, S.-W.; Son, S. U.; Lee, S. I.; Hyeon, T.; Chung, Y. K. *J. Am. Chem. Soc.* **2000**, *122*, 1550.
(16) Han, Y.-J.; Stucky, G. D.; Butler, A. *J. Am. Chem. Soc.* **1999**, *121*, 9897.
(17) Bae, S. J.; Kim, S.-W.; Hyeon, T.; Kim, B. M. *Chem. Commun.* **1999**, 31.
(18) Lin, H.-P.; Yang, L.-Y.; Mou, C.-Y.; Liu, S.-B.; Lee, H.-K. *New J. Chem.* **2000**, *24*, 253.
(19) Liu, A. M.; Hidajat, K.; Kawi, S.; Zhao, D. Y. *Chem. Commun.* **2000**, 1145.
(20) Liu, J.; Shin, Y.; Nie, Z.; Chang, J. H.; Wang, L.-Q.; Fryxell, G. E.; Samuels, W. D.; Exarhos, G. J. *J. Phys. Chem. A* **2000**, *104*, 8328.
(21) Washmon-Kriel, L.; Jimenez, V. L.; Balkus, K. J. *J. Mol. Catal. B—Enzymatic* **2000**, *10*, 453.
(22) Yang, P.; Wirnsberger, G.; Huang, H. C.; Cordero, S. R.; McGehee, M. D.; Scott, B.; Deng, T.; Whitesides, G. M.; Chmelka, B. F.; Buratto, S. K.; Stucky, G. D. *Science* **2000**, *287*, 465.
(23) Wirnsberger, G.; Scott, B. J.; Chmelka, B. F.; Stucky, G. D. *Adv. Mater.* **2000**, *12*, 1450.
(24) Doshi, D. A.; Huesing, N. K.; Lu, M.; Fan, H.; Lu, Y.; Simmons-Potter, K.; Potter, B. G., Jr.; Hurd, A. J.; Brinker, C. J. *Science* **2000**, *290*, 107.
(25) Wirnsberger, G.; Scott, B. J.; Stucky, G. D. *Chem. Commun.* **2001**, 119.
(26) Huang, M. H.; Choudrey, A.; Yang, P. *Chem. Commun.* **2000**, 1063.
(27) Han, Y.-J.; Kim, J. M.; Stucky, G. D. *Chem. Mater.* **2000**, *12*, 2068.
(28) Kang, H.; Jun, Y.-w.; Park, J.-I.; Lee, K.-B.; Cheon, J. *Chem. Mater.* **2000**, *12*, 3530.
(29) Shin, H. J.; Ko, C. H.; Ryoo, R. *J. Mater. Chem.* **2001**, *11*, 260.
(30) Ryoo, R.; Ko, C. H.; Kruk, M.; Antochshuk, V.; Jaroniec, M. *J. Phys. Chem. B* **2000**, *104*, 11465.
(31) Jun, S.; Joo, S. H.; Ryoo, R.; Kruk, M.; Jaroniec, M.; Liu, Z.; Ohsuna, T.; Terasaki, O. *J. Am. Chem. Soc.* **2000**, *122*, 10712.
(32) Coleman, N. R. B.; Morris, M. A.; Spalding, T. R.; Holmes, J. D. *J. Am. Chem. Soc.* **2001**, *123*, 187.
(33) Jang, J.; Lim, B.; Lee, J.; Hyeon, T. *Chem. Commun.* **2001**, 83.
(34) Kwon, O.-Y.; Kim, S.; Choi, S.-W. *Microporous Mesoporous Mater.* **1999**, *27*, 255.
(35) Newalkar, B. L.; Olanrewaju, J.; Komarneni, S. *Chem. Mater.* **2001**, *13*, 552.
(36) Newalkar, B. L.; Komarneni, S.; Katsuki, H. *Chem. Commun.* **2000**, 2389.
(37) Sierra, L.; Guth J.-L. *Microporous Mesoporous Mater.* **1999**, *27*, 243.
(38) Kim, S.-S.; Pauly, T. R.; Pinnavaia, T. J. *Chem. Commun.* **2000**, 835.
(39) Boissiere, C.; Larbot, A.; Prouzet, E. *Chem. Mater.* **2000**, *12*, 1937.
(40) Prouzet, E.; Pinnavaia, T. J. *Angew. Chem., Int. Ed. Engl.* **1997**, *36*, 516.
(41) Kim, J. M.; Stucky, G. D. *Chem. Commun.* **2000**, 1159.
(42) Schmidt-Winkel, P.; Lukens, W. W., Jr.; Zhao, D.; Yang, P.; Chmelka, B. F.; Stucky, G. D. *J. Am. Chem. Soc.* **1999**, *121*, 254.
(43) Sing, K. S. W.; Everett, D. H.; Haul, R. A. W.; Moscou, L.; Pierotti, R. A.; Rouquerol, J.; Siemieniewska, T. *Pure Appl. Chem.* **1985**, *57*, 603.
(44) Sayari, A.; Liu, P.; Kruk, M.; Jaroniec, M. *Chem. Mater.* **1997**, *9*, 2499.
(45) Jaroniec, M.; Kruk, M.; Olivier, J. P. *Langmuir* **1999**, *15*, 5410.
(46) Kruk, M.; Jaroniec, M.; Sayari, A. *Langmuir* **1997**, *13*, 6267.
(47) Kruk, M.; Jaroniec, M.; Sayari, A. *Chem. Mater.* **1999**, *11*, 492.
(48) Kruk, M.; Jaroniec, M.; Ko, C. H.; Ryoo, R. *Chem. Mater.* **2000**, *12*, 1961.
(49) Shin, H. J.; Ryoo, R.; Kruk, M.; Jaroniec, M. *Chem. Commun.* **2001**, 349.
(50) Beck, J. S.; Vartuli, J. C.; Roth, W. J.; Leonowicz, M. E.; Kresge, C. T.; Schmitt, K. D.; Chu, C. T—W.; Olson, D. H.; Sheppard, E. W.; McCullen, S. B.; Higgins, J. B.; Schlenker, J. L. *J. Am. Chem. Soc.* **1992**, *114*, 10834.
(51) Matos, J. R.; Mercuri, L. P.; Kruk, M.; Jaroniec, M. *Chem. Mater.* **2001**, *13*, 1726.
(52) Pauly, T. R.; Pinnavaia, T. J. *Chem. Mater.* **2001**, *13*, 987.
(53) Smarsly, B.; Goltner, C.; Antonietti, M.; Ruland, W.; Hoinkis, E. *J. Phys. Chem. B* **2001**, *105*, 831.
(54) Stroud, W. J.; Curry, J. E.; Cushman, J. H. *Langmuir* **2001**, *17*, 688.